

## Uranium Tris-aryloxide Derivatives Supported by Triazacyclononane: Engendering a Reactive Uranium(III) Center with a Single Pocket for Reactivity

Ingrid Castro-Rodriguez, Kristian Olsen, Peter Gantzel, and Karsten Meyer\*

Contribution from the Department of Chemistry and Biochemistry, University of California, San Diego, 9500 Gilman Drive MC 0358, La Jolla, California 92093-0358

Received August 29, 2002; E-mail: kmeyer@ucsd.edu

**Abstract:** The synthesis and spectroscopic characterization of the mononuclear uranium complex  $[(\text{ArO})_3\text{tacn}]\text{U}^{\text{III}}(\text{NCCH}_3)$  is reported. The uranium(III) complex reacts with organic azides to yield uranium(IV) azido as well as uranium(V) imido complexes,  $[(\text{ArO})_3\text{tacn}]\text{U}^{\text{IV}}(\text{N}_3)$  and  $[(\text{ArO})_3\text{tacn}]\text{U}^{\text{V}}(\text{NSi}(\text{CH}_3)_3)$ . Single-crystal X-ray diffraction, spectroscopic, and computational studies of this analogous series of uranium tris-aryloxide complexes supported by triazacyclononane are described. The hexadentate, tris-anionic ligand coordinates to the large uranium ion in unprecedented fashion, engendering coordinatively unsaturated and highly reactive uranium centers. The macrocyclic triazacyclononane tris-aryloxide derivative occupies six coordination sites, with the three aryloxide pendant arms forming a trigonal plane at the metal center. DFT quantum mechanic methods were applied to rationalize the reactivity and to elucidate the electronic structure of the newly synthesized compounds. It is shown that the deeply colored uranium(III) and uranium(V) species are stabilized via  $\pi$ -bonding interaction, involving uranium f-orbitals and the axial acetonitrile and imido ligand, respectively. In contrast, the bonding in the colorless uranium(IV) azido complex is purely ionic in nature. The magnetism of the series of complexes with an  $[\text{N}_3\text{O}_3\text{-N}_{ax}]$  core structure and oxidation states +III, +IV, and +V is discussed in context of the electronic structures.

### Introduction

While bonding in f-elements is traditionally described as mainly electrostatic, the issue of covalency remains an important subject of debate.<sup>1–3</sup> To elucidate fundamental questions regarding trends in bonding and reactivity in uranium and other actinide metal compounds, the detailed investigation and discovery of unprecedented species is necessary. In our efforts to identify and isolate new uranium complexes with enhanced reactivity relevant to binding, activation, and functionalization of small molecules, we are currently investigating the coordination chemistry of uranium metal centers with classical Werner-type ligands. The stabilizing abilities of “classic” macrocyclic amines have made this class of chelators an indispensable tool for transition metal coordination chemistry. However, to the best of our knowledge, uranium complexes of macrocyclic polyamine ligands have not yet been reported in the literature.

Here we report uranium (III, IV, and V) tris-aryloxide derivatives supported by triazacyclononane to demonstrate that the coordinated ligand provides an unprecedented platform for enhanced uranium reactivity. The introduction of the functionalized triazacyclononane ligand, 1,4,7-tris(3,5-di-*tert*-butyl-2-hydroxybenzyl)-1,4,7-triazacyclononane,<sup>4</sup> to a uranium(III) metal

center results in the formation of stable core complexes with only one reactive coordination site. The ancillary ligand occupies six coordination sites, leaving the seventh, an axial position, available for ligand substitution reactions and redox events associated with small molecule or organic functional group activation. This coordination mode to uranium is distinctly different from that observed for binding to transition metals with which the ligand forms exclusively coordinatively saturated octahedral complexes.<sup>5–11</sup>

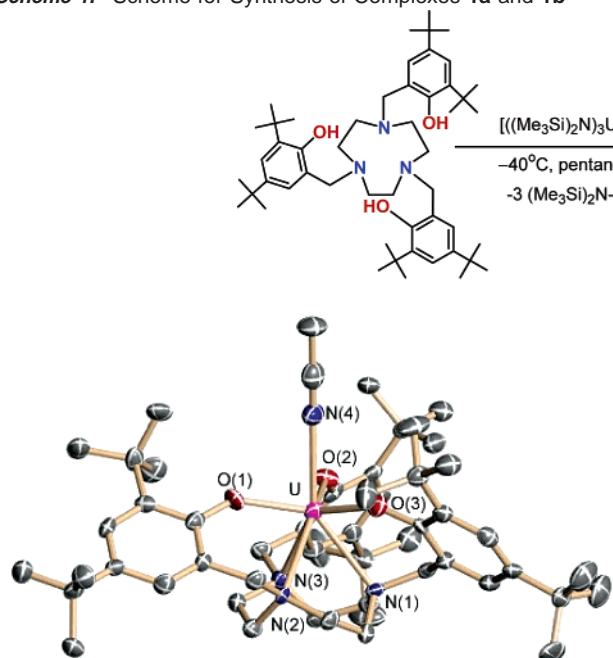
The in-depth crystallographic and spectroscopic characterization along with a computational study to investigate the electronic structure of this new class of uranium complexes is presented herein.

### Results and Discussion

**Synthesis and Molecular Structure of 1b.** Treatment of  $[\text{U}(\text{N}(\text{Si}(\text{CH}_3)_2)_3)]^{12,13}$  with 1 equiv of 1,4,7-tris(3,5-di-*tert*-

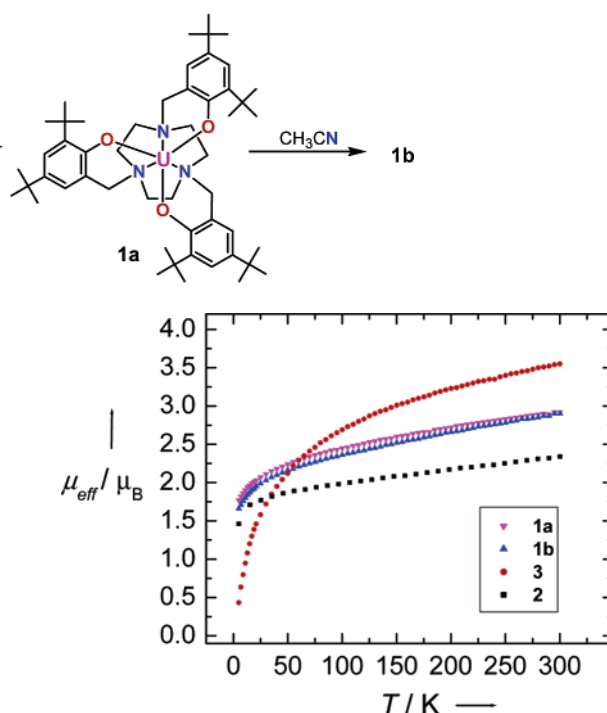
(1) Diaconescu, P. L.; Arnold, P. L.; Baker, T. A.; Mindiola, D. J.; Cummins, C. C. *J. Am. Chem. Soc.* **2000**, *122*, 6108–6109.  
(2) Meyer, K.; Mindiola, D. J.; Baker, T. A.; Davis, W. M.; Cummins, C. C. *Angew. Chem., Int. Ed.* **2000**, *39*, 3063–3066.  
(3) Mazzanti, M.; Wietzke, R. L.; Pecaut, J.; Latour, J. M.; Maldivi, P.; Remy, M. *Inorg. Chem.* **2002**, *41*, 2389–2399.

(4) Chaudhuri, P.; Wieghardt, K. *Progress in Inorganic Chemistry*; John Wiley & Sons: New York, 2001; Vol. 50, pp 151–216.  
(5) Adam, B.; Bill, E.; Bothe, E.; Goerd, B.; Haselhorst, G.; Hildenbrand, K.; Sokolowski, A.; Steenken, S.; Weyhermuller, T.; Wieghardt, K. *Chem.-Eur. J.* **1997**, *3*, 308–319.  
(6) Auerbach, U.; Eckert, U.; Wieghardt, K.; Nuber, B.; Weiss, J. *Inorg. Chem.* **1990**, *29*, 938–944.  
(7) Auerbach, U.; Stockheim, C.; Weyhermuller, T.; Wieghardt, K.; Nuber, B. *Angew. Chem., Int. Ed. Engl.* **1993**, *32*, 714–716.  
(8) Auerbach, U.; Weyhermuller, T.; Wieghardt, K.; Nuber, B.; Bill, E.; Butzlaff, C.; Trautwein, A. X. *Inorg. Chem.* **1993**, *32*, 508–519.  
(9) Snodin, M. D.; Ould-Moussa, L.; Wallmann, U.; Lecomte, S.; Bachler, V.; Bill, E.; Hummel, H.; Weyhermuller, T.; Hildebrandt, P.; Wieghardt, K. *Chem.-Eur. J.* **1999**, *5*, 2554–2565.  
(10) Sokolowski, A.; Bothe, E.; Bill, E.; Weyhermuller, T.; Wieghardt, K. *Chem. Commun. (Cambridge, U.K.)* **1996**, 1671–1672.

**Scheme 1.** Scheme for Synthesis of Complexes **1a** and **1b****Figure 1.** Molecular structure of  $[(\text{ArO})_3\text{tacn}]\text{U}(\text{NCCH}_3)_2$  in crystals of **1b**·2CH<sub>3</sub>CN. Selected hydrogen atoms and cocrystallized solvent molecules are omitted for clarity.

butyl-2-hydroxybenzyl)-1,4,7-triazacyclononane<sup>4</sup> ((ArOH)<sub>3</sub>tacn) in pentane yields a reactive uranium(III) species  $[(\text{ArO})_3\text{tacn}]\text{U}$  (**1a**) on a multigram scale (70% recrystallized yield) as a red-brown crystalline substance (Scheme 1).

Recrystallization of **1a** from acetonitrile at  $-40^\circ\text{C}$  yields the purple crystalline compound  $[(\text{ArO})_3\text{tacn}]\text{U}(\text{NCCH}_3)_2$  (**1b**) in approximately 90% yield. An X-ray diffraction study on single crystals of **1b** reveals an axial acetonitrile molecule in the coordination sphere of the seven-coordinate uranium species (Figure 1). The coordination polyhedron can best be described as a distorted tricapped tetrahedron with the triazacyclononane fragment and the monodentate ligand forming the tetrahedron and the trigonal planar aryloxides capping three faces. Three coordinating anionic aryloxy oxygen atoms compensate the formal +III charge of the uranium ion. The average U–O distance was determined to be 2.26 Å. The triazacyclononane fragment occupies the position trans to the acetonitrile ligand. The uranium metal center is displaced 0.442 Å out of the trigonal plane formed by the three oxygens toward the nine-membered polyamine ligand. It is noteworthy that the U–N(CH<sub>3</sub>CN) bond distance at 2.66 Å is slightly shorter than the average U–N(tacn) bond length of 2.70 Å. This weak but significant U–N(tacn) interaction, and the pronounced tendency of uranium to bind hard and anionic donor ligands in a trigonal planar fashion, results in an increased average dihedral angle N–CH<sub>2</sub>–C<sub>ar1</sub>–C<sub>ar2</sub> of 62.4° (59.13, 60.53, 67.63°) of the aryloxy pendant arms as compared to 50.75° in octahedral [L<sup>Bu</sup>Cr] (L<sup>Bu</sup> = 1,4,7-tris(3-*tert*-butyl-2-hydroxybenzyl)-1,4,7-triazacyclononane).<sup>8</sup>

**Figure 2.** Temperature dependence of the effective magnetic moment  $\mu_{\text{eff}}$  of solid samples of **1a**, **1b**, **2**, and **3**.

The unique coordination mode of this ligand to the large uranium ion makes this ligand an attractive chelator for the stabilization of coordinatively unsaturated, reactive species. The *tert*-butyl substituents of the aryloxy ligands form a protective cavity around the CH<sub>3</sub>CN, which is the reactive site of this system as evidenced by the reactivity studies described below. Undesired side reactions trans to the reactive site are eliminated due to shielding by the triazacyclononane fragment.

The <sup>1</sup>H NMR spectra of **1a** and **1b** recorded in C<sub>6</sub>D<sub>6</sub> are very similar: In the spectrum of **1b**, two resonances at 2.28 and 4.11 ppm can be readily assigned to the *tert*-butyl groups but are high-field shifted as compared to **1a** (2.63 and 4.15 ppm). Eight more resonances between  $-25$  and 20 ppm integrate properly. Although the assignment remains largely equivocal, their position is diagnostic in determining the purity and stability of **1a** and **1b** in solution. The protons of the coordinated acetonitrile molecule in **1b** cannot be detected. This likely is due to signal broadening resulting from their close proximity and relatively strong binding to the paramagnetic uranium center (vide infra).

**Magnetism of 1b.** SQUID magnetization measurements were carried out to study the temperature behavior of the trivalent uranium species **1a** and **1b**. The temperature behaviors as well as the magnetic moments of **1b** are remarkably similar to those of the analogous six-coordinate precursor molecule **1a** (Figure 2).

Complex **1b** displays a strong temperature-dependent magnetic moment, varying from 1.66  $\mu_{\text{B}}$  at 4 K to 2.90  $\mu_{\text{B}}$  at room temperature. This magnetic moment of 2.90  $\mu_{\text{B}}$  at room temperature, however, is significantly smaller than the expected moment of  $\mu_{\text{B}}(\text{calcd}) = 3.62 \mu_{\text{B}}$  for an f-element species with three unpaired electrons and full spin–orbit coupling (Russell–Saunders term: <sup>4</sup>I<sub>9/2</sub>). Accordingly, measurements were carried out in the temperature range between 5 and 350 K, to study whether samples of **1b** reach saturation magnetization at elevated

(11) Sokolowski, A.; Muller, J.; Weyhermüller, T.; Schnepf, R.; Hildebrandt, P.; Hildenbrand, K.; Bothe, E.; Wieghardt, K. *J. Am. Chem. Soc.* **1997**, *119*, 8889–8900.

(12) Clark, D. L.; Sattelberger, A. P.; Andersen, R. A. *Inorg. Synth.* **1997**, *31*, 307–315.

(13) Stewart, J. L.; Andersen, R. A. *Polyhedron* **1998**, *17*, 953–958.

**Table 1.** Mulliken Populations for  $[((\text{ArO})_3\text{tacn})\text{U}(\text{NCCH}_3)]^a$ 

atom	charge	spin-density	spin	S	P	D	F
U	1.6775	2.8753	$\alpha$	1.1356	2.9571	0.7366	2.7696
			$\beta$	1.0529	2.9133	0.4637	0.2937
$\text{O}_{\text{av}}$	−0.7050	−0.0429	$\alpha$	0.9362	2.3697	0.0252	0.0000
			$\beta$	0.9374	2.4107	0.0234	0.0000
$\text{N}_{\text{tacn,av}}$	−0.5021	−0.0130	$\alpha$	0.7979	1.9063	0.0402	0.0000
			$\beta$	0.8005	1.9176	0.0394	0.0000
$\text{N}_{\text{CH}_3\text{CN}}$	−0.2081	0.0006	$\alpha$	0.8184	1.7535	0.0324	0.0000
			$\beta$	0.8316	1.7491	0.0231	0.0000
$\text{C}_{\text{CH}_3\text{CN}}$	0.1539	0.2535	$\alpha$	0.2535	1.3580	0.0374	0.0000
			$\beta$	0.6342	1.1250	0.0371	0.0000

<sup>a</sup> For electronically equivalent atoms, mean values are given.

temperatures corresponding to the expected value for an  $f^3$  ion. It was found that the magnetic moment continuously increases to  $3.40 \mu_B$  at 350 K and does not reach a plateau at this temperature.<sup>14</sup> The observed reduced magnetic moment is likely due to a significant degree of covalency in the uranium(III) species, quenching spin–orbit coupling and thus reducing the magnetic moment (vide infra).

**Electronic Structure of 1b.** The electronic structure of **1b** was studied using force-field methods and density functional theory calculations. Because of the low symmetry in **1b**, the coordinates of the diffraction analysis were taken as a starting point for the geometry optimization. The calculation converged in straightforward fashion, resulting in structural parameters within  $3\sigma$  of the experimentally determined structure. Electrons 1–3, the three most energetic electrons of the system, were found to be uranium based (2.88 of the total spin density, see Table 1 (Mulliken population)). Analysis of these frontier orbitals (Figure 3) reveals the origin of the relatively short U–N(CH<sub>3</sub>CN) bond. SOMO–1 is almost a pure f-orbital. Its shape resembles those of the  $x(x^2 - y^2)$  and  $x(3x^2 - y^2)$  orbitals in a general set of f-orbitals and is antibonding with respect to the phenolate oxygen ligands. With respect to SOMO–1, SOMO–2 and SOMO–3 are slightly more stabilized (by 7.2 kJ/mol) via a  $\pi$ -back-bonding interaction with the apical acetonitrile ligand and almost doubly degenerate ( $\Delta(\text{SOMO–2} - \text{SOMO–3}) = 1.14$  kJ/mol). Interestingly, close examination of the total electron density in **1b** also shows that one of the three amine nitrogen donor atoms possesses a higher degree of U–N interaction than the remaining two, resulting in one U–N(tacn) bond distance (2.665(6) Å) that is significantly shorter than the other two (2.715(6) and 2.721(5) Å).

Uranium(III) species **1a** and **1b**, with an open or masked coordination site at a reactive, low-valent uranium center, represent important precursor molecules to explore new modes of uranium reactivity. Few uranium complexes involving U–N multiple bonds have been described in the literature; however, isolation of a molecular uranium nitrido species remains elusive.<sup>8–10</sup> Given the paucity of structural and reactivity studies of complexes with uranium nitrogen multiple bonds, synthesis, isolation, and characterization of novel potent uranium nitrido precursor compounds are important objectives of this research and are described in the following sections.

**Synthesis and Molecular Structure of 2 and 3.** Treatment of **1a** with 1 equiv of trimethylsilyl azide has been found to

(14) Samples of **1b** do not decompose at elevated temperature under an inert-gas atmosphere. Analyses were performed in triplicate using different preparations of the compounds. Compound integrity was checked by <sup>1</sup>H NMR and elemental analysis after the magnetization measurements.

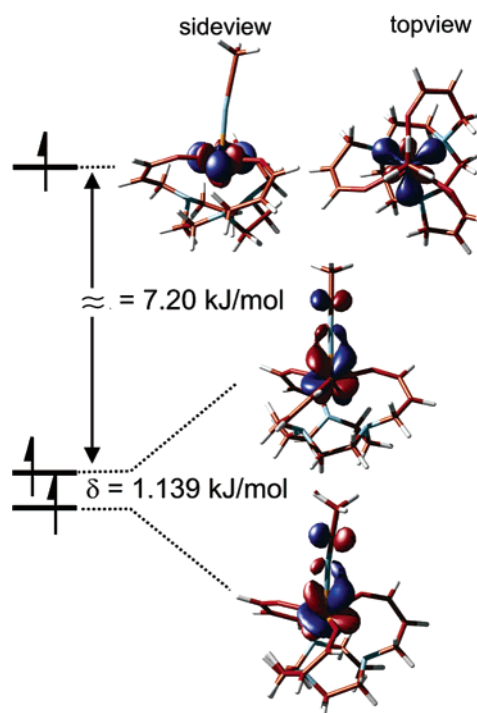


**Figure 3.** Molecular orbitals depicted for the three most energetic electrons in the system of **1b**: SOMO–1 (top), SOMO–2/3 (middle and bottom).

form the green uranium(V) imido complex  $[((\text{ArO})_3\text{tacn})\text{U}(\text{N}(\text{Si}(\text{CH}_3)_3))] (\mathbf{2})$  with evolution of dinitrogen and a colorless uranium(IV) azido species  $[((\text{ArO})_3\text{tacn})\text{U}(\text{N}_3)] (\mathbf{3})$  as a side product. Compound **3** with an  $\eta^1$ -coordinated azido ligand can be obtained reproducibly by providing the organic trityl azide as the source of the azido radical oxidizing the uranium(III) center. In contrast, 1-adamantyl azide (Ad–N<sub>3</sub>) produces the uranium(V) imido species  $[((\text{ArO})_3\text{tacn})\text{U}(\text{N}(\text{Ad}))] (\mathbf{2b})$  exclusively.

Structural data for compounds **2** and **3** were obtained by single-crystal X-ray diffraction analysis. Complex **2** crystallizes with two independent molecules per asymmetric unit. The solid-state molecular structures of one of the two independent molecules in crystals of **2** and complex **3** are depicted in Figure 4. Selected bond distances and angles for **1b**, **2**, and **3** are summarized in Table 2.

The formation of an imido complex results in oxidation of the trivalent uranium center of precursor **1b** to a formally pentavalent uranium(V) ion in complex **2**. Accordingly, the average uranium–oxygen bond distance decreases from 2.265 Å in **1b** to 2.189 and 2.203 Å in **2**. A small number of uranium–(IV), (V), and (VI) imido and bis-imido species  $[\text{U}\equiv\text{N}-\text{R}]$  with R = alkyl, aryl, NNPh<sub>2</sub> have been described in the literature.<sup>1,15–22</sup> Reported U–N bond distances in mononuclear imido complexes

(15) Zalkin, A.; Brennan, J. G.; Andersen, R. A. *Acta Crystallogr., Sect. C: Cryst. Struct. Commun.* **1988**, *44*, 1553–1554.

(16) Burns, C. J.; Smith, W. H.; Huffman, J. C.; Sattelberger, A. P. *J. Am. Chem. Soc.* **1990**, *112*, 3237–3239.

(17) Arney, D. S. J.; Burns, C. J. *J. Am. Chem. Soc.* **1995**, *117*, 9448–9460.

(18) Warner, B. P.; Scott, B. L.; Burns, C. J. *Angew. Chem., Int. Ed.* **1998**, *37*, 959–960.

(19) Peters, R. G.; Warner, B. P.; Burns, C. J. *J. Am. Chem. Soc.* **1999**, *121*, 5585–5586.

(20) Peters, R. G.; Warner, B. P.; Scott, B. L.; Burns, C. J. *Organometallics* **1999**, *18*, 2587–2589.

(21) Duval, P. B.; Burns, C. J.; Buschmann, W. E.; Clark, D. L.; Morris, D. E.; Scott, B. L. *Inorg. Chem.* **2001**, *40*, 5491–5496.

(22) Kiplinger, J. L.; Morris, D. E.; Scott, B. L.; Burns, C. J. *Chem. Commun. (Cambridge, U. K.)* **2002**, 30–31.



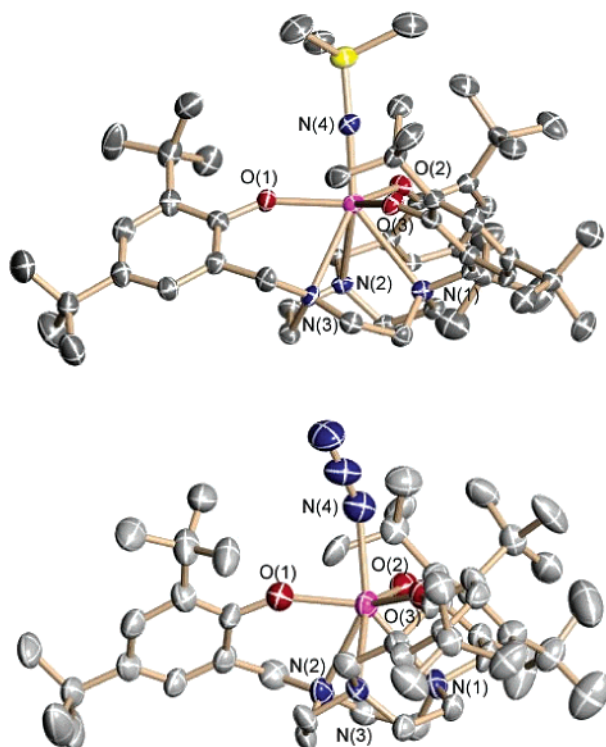


**Figure 4.** Solid-state molecular structures of  $[(\text{ArO})_3\text{tacn})\text{U}(\text{NSi}(\text{CH}_3)_3)]$  and  $[(\text{ArO})_3\text{tacn})\text{U}(\text{N}_3)]$  in crystals of  $2 \cdot \text{C}_6\text{H}_{14}$  (top) and  $3 \cdot \text{C}_6\text{H}_{14}$  (bottom). Only one of the two independent molecules in crystals of **2** is shown. Hydrogen atoms and cocrystallized hexane solvent molecules are omitted for clarity.

**Table 2.** Selected Structural Parameters for Complexes **1b**, **2**, and **3** (Bond Distances in Å, Bond Angles in deg)

structural parameters	1b	2	3
U–N <sub>1tacn</sub>	2.662(6)	2.719(5)/2.791(4)	2.825(9)
U–N <sub>2tacn</sub>	2.721(5)	2.737(5)/2.724(4)	2.758(9)
U–N <sub>3tacn</sub>	2.715(6)	2.660(5)/2.735(4)	2.886(9)
U–N <sub>av</sub>	2.70	2.70/2.75	2.83
U–O <sub>1ArO</sub>	2.265(5)	2.196(4)/2.161(4)	2.294(8)
U–O <sub>2ArO</sub>	2.271(5)	2.203(4)/2.185(4)	2.295(8)
U–O <sub>3ArO</sub>	2.258(5)	2.209(4)/2.222(4)	2.286(8)
U–O <sub>av</sub>	2.26	2.20/2.19	2.29
U–N <sub>CH<sub>3</sub>CN</sub>	2.663(7)		
U–N <sub>azido</sub>			2.564(12)
U–N <sub>imido</sub>		1.985(5)/1.992(4)	
U <sub>out-of-plane shift</sub>	0.442	0.151	0.308
U–N–C <sub>CH<sub>3</sub>CN</sub>	167.1(7)		
U–N–Si <sub>imido</sub>		178.5(3)/168.9(3)	
U–N <sub>α</sub> –N <sub>β</sub>			145.6(9)

vary from 1.90 to 2.05 Å, and [U–N–R] angles are found ranging from 170 to 180°. Observation of short U–N(imido) bond distances together with near linear [U–N–R] angles has been described as being indicative of multiple bonds between the uranium and nitrogen atom, with both nitrogen lone pairs donating into e-symmetry uranium f-orbitals to form a formal U–N triple bond.<sup>23</sup> The uranium–imido bond in **2** also exhibits significant  $\pi$ -bonding as evidenced by the short U–N(imido) bond distance of 1.991(4) and 1.985(5) Å and an almost linear U–N–Si(CH<sub>3</sub>)<sub>3</sub> entity ( $\angle\text{U–N–Si} = 168.9(3)$  and  $178.5(3)^\circ$ ). To achieve efficient  $\pi$ -overlap with the apical trimethylsilyl imido group, the uranium ion shifts closer to the plane formed by the three oxygen atoms, resulting in an out-of-plane shift of

(23) Brennan, J. G.; Andersen, R. A. *J. Am. Chem. Soc.* **1985**, *107*, 514–516.

0.126 and 0.177 Å, respectively. Despite this shift away from the triazacyclononane nitrogen atoms, the average U–N(tacn) distance of 2.70 Å in **1b** remains unchanged as compared to that in molecules of **2** (2.75 and 2.70 Å), confirming a bonding interaction with the tacn-amine nitrogens.

The uranium(IV) azide species in crystals of **3** displays significantly longer average U–N(tacn) and U–OAr bond distances at 2.83 and 2.29 Å, respectively. The uranium center in **3** is placed 0.308 Å below the plane of the three aryloxy oxygens, which is close to the mathematical average of 0.297 Å of the displacement in complexes **1b** and **2** with oxidation states +III and +V. The linear azide ligand ( $\text{N}_\alpha\text{–N}_\beta\text{–N}_\gamma = 178.2(14)^\circ$ ) coordinates with an angle of  $145.9(9)^\circ$  to the uranium center. The uranium–azide bond distance was determined to be 2.562(12) Å. Structurally characterized uranium azido complexes are rare. With the exception of one mononuclear uranyl complex involving a terminal azide ligand ( $d(\text{U–N}_\alpha) = 2.382$  Å,  $\angle(\text{U–N}_\alpha\text{–N}_\beta) = 131.67^\circ$ )<sup>24</sup> and a small number of polynuclear uranyl complexes with terminal and bridged azido ligands,<sup>25</sup> only one other crystallographically characterized U(III) azido species is reported in the literature.<sup>26</sup> The U–N<sub>α</sub> bond distances in the dinuclear 1,3- $\mu$ -azido bridged tris-trimethylsilylcyclopentadienyl uranium anion were found equidistant at 2.40(2) Å with a U–N<sub>α</sub>–N<sub>β</sub> angle of  $160(1)^\circ$  (inversion center on N<sub>β</sub>).

An interesting question arising from the structural investigation of compounds **1b**, **2**, and **3** is to what extent the polyamine macrocycle is coordinated to the uranium center. Is the triazacyclononane ligand an effective chelator, or is the macrocycle merely held in place by the coordinating phenolate pendant arms? Uranium species such as  $[(\text{N}_3\text{N})\text{U}(\text{X})]$  (X = Cl, Br, I)<sup>27</sup> and  $[(\text{N}_3\text{N}')\text{U}]_2(\mu\text{-L})]$  (L = N<sub>2</sub>, Cl, (N<sub>3</sub>N' = N(CH<sub>2</sub>–CH<sub>2</sub>NSiBu<sup>t</sup>Me<sub>2</sub>)<sub>3</sub>)<sup>28,29</sup>) are species with tris-anionic pendant arms and a single-nitrogen amine anchor.<sup>30</sup> For these complexes, U–N<sub>amine</sub> bond distances vary from 2.644 to 2.685 Å in the mononuclear and from 2.553 to 2.775 Å in the dinuclear complexes. A uranium compound with a neutral ethylenediamine ligand [(TMED)<sub>2</sub>U(Cl)<sub>4</sub>] (TMED = tetramethylethylenediamine) by Anderson et al. is the only other reported amine complex and represents an important complex for comparison.<sup>31</sup> The average uranium–amine bond distances in this uranium(IV) species were determined at  $d(\text{U–N}_{\text{av}}) = 2.79$  Å, slightly shorter than the U–N(tacn) bond lengths in **3** (2.82 Å), but significantly longer than the corresponding bonds in **1b** and **2** (2.70 Å), indicating bonding interactions of the macrocyclic amine ligands with the uranium center.

**Electronic Structure and Magnetism of 2 and 3.** The complexes  $[(\text{ArO})_3\text{tacn})\text{U}(\text{L})]$  with L = CH<sub>3</sub>CN, N<sub>3</sub><sup>–</sup>, ((CH<sub>3</sub>)<sub>3</sub>Si)–N<sub>2</sub><sup>–</sup> described in this report provide a unique opportunity to study the electronic properties of this novel series of uranium

(24) Prasad, L.; Gabe, E. J.; Glavincevski, B.; Brownstein, S. *Acta Crystallogr., Sect. C: Cryst. Struct. Commun.* **1983**, *39*, 181–184.

(25) Charpin, P.; Lance, M.; Nierlich, M.; Vigner, D.; Livet, J.; Musikas, C. *Acta Crystallogr., Sect. C: Cryst. Struct. Commun.* **1986**, *42*, 1691–1694.

(26) Berthet, J. C.; Lance, M.; Nierlich, M.; Vigner, J.; Ephritikhine, M. *J. Organomet. Chem.* **1991**, *420*, C9–C11.

(27) Roussel, P.; Alcock, N. W.; Boaretto, R.; Kingsley, A. J.; Munslow, I. J.; Sanders, C. J.; Scott, P. *Inorg. Chem.* **1999**, *38*, 3651–3656.

(28) Roussel, P.; Scott, P. *J. Am. Chem. Soc.* **1998**, *120*, 1070–1071.

(29) Roussel, P.; Hitchcock, P. B.; Tinker, N.; Scott, P. *Chem. Commun. (Cambridge, U. K.)* **1996**, 2053–2054.

(30) Cummins, C. C.; Lee, J.; Schrock, R. R.; Davis, W. D. *Angew. Chem., Int. Ed. Engl.* **1992**, *31*, 1501–1503.

(31) Zalkin, A.; Edwards, P. G.; Zhang, D.; Andersen, R. A. *Acta Crystallogr., Sect. C: Cryst. Struct. Commun.* **1986**, *42*, 1480–1482.

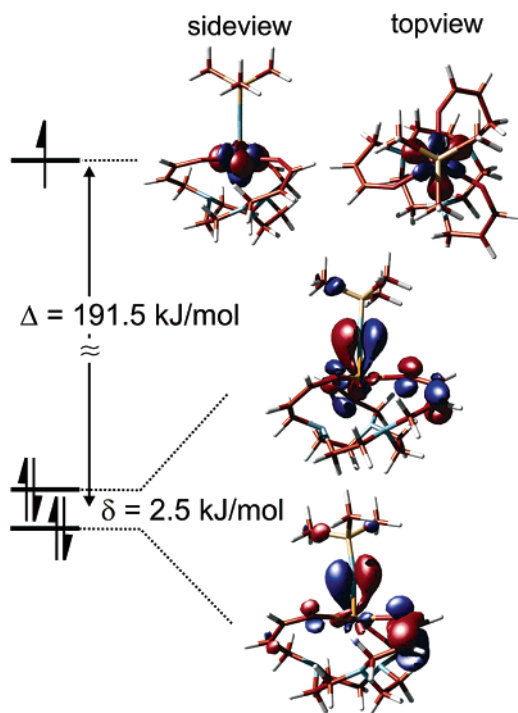


**Figure 5.** Molecular orbitals depicted for the five most energetic electrons in the system of **2**: SOMO–1 (top), HOMO–2/3 (middle and bottom).

**Table 3.** Mulliken Populations for  $[(\text{ArO})_3\text{tacn}]\text{U}(\text{NSi}(\text{CH}_3)_3)^a$

atom	charge	spin-density	spin	S	P	D	F
U	1.8159	1.2222	$\alpha$	1.0885	2.9465	0.8044	1.8638
			$\beta$	1.0667	2.9319	0.6674	0.8149
$\text{O}_{\text{av}}$	−0.6537	−0.0265	$\alpha$	1.9104	2.3777	0.0257	0.0000
			$\beta$	1.9122	2.4032	0.0247	0.0000
$\text{N}_{\text{tacn}_{\text{av}}}$	−0.5583	−0.0101	$\alpha$	1.7867	1.9467	0.0407	0.0000
			$\beta$	1.7884	1.9555	0.0403	0.0000
$\text{N}_{\text{TMS}}$	−0.7781	−0.0964	$\alpha$	1.8637	1.9672	0.0099	0.0000
			$\beta$	1.8666	2.0611	0.0096	0.0000

<sup>a</sup> For electronically equivalent atoms, mean values are given.

species. The formal oxidation states vary from +III (**1b**) to +IV and +V (**2** and **3**), respectively, with the core structure  $[(\text{ArO})_3\text{tacn}]\text{U}$  unchanged throughout this series.

DFT calculations on **1b**, **2** (Figure 5), and **3** show that the coordination geometry of the hexadentate aryloxide functionalized triazacyclononane ligand has an electronic origin and is not a result of steric effects imposed by the six *tert*-butyl groups, for instance. In all three molecules, strong  $\sigma$  interactions to the three aryloxide oxygens are observed. In contrast, the U–N(tacn) interactions are almost purely electrostatic in nature. While complexes **1b** and **2** display significant  $\pi$ -bonding involving f-type uranium orbitals and  $\pi$ -orbitals of the axial acetonitrile and imido ligand, respectively, bonding in compound **3** is almost purely electrostatic, exhibiting no  $\pi$ -interaction with the apical azide ligand. This is also confirmed by the Mulliken population summarized in Tables 1 and 3 (for Mulliken population and energy diagram of **3**, see Supporting Information Table S1 and Figure S1). On the basis of the orbital diagram and the Mulliken population analysis, it is evident that there is no covalency in the polyamine nitrogen–uranium bonds.

The U(IV) ion in **3** has a  $5f^2$  electron configuration and a nominal  $^3\text{H}_4$  ground level. The magnetic moment of **3** varies from 0.4 at 5 K to  $3.55 \mu_{\text{B}}$  at 300 K (Figure 2). The paramag-

netism at room temperature is in good agreement with the theoretically determined free ion moment of  $\mu_{\text{eff}} = g_f(J(J + 1))^{1/2} = 3.58 \mu_{\text{B}}$ , but interestingly is significantly *higher* than that found in samples of uranium(III)  $f^3$  species **1a** and **1b**.<sup>32</sup> This is in good agreement with the calculated results for the electronic structure of **3** displaying almost no covalent metal–ligand interactions. Accordingly, this purely ionic species displays “normal” f-element magnetism.

Samples of **2**, however, display a much smaller magnetic moment of  $\mu_{\text{eff}} = 2.34 \mu_{\text{B}}$  at 300 K that varies with the temperature, reaching an effective moment of  $\mu_{\text{eff}} = 1.46 \mu_{\text{B}}$  at 5 K (Figure 2). It is known that magnetic properties of U(V)  $f^1$  systems vary considerably depending on the nature of the ligands and the geometry. In most instances, however, the observed magnetic moments are reduced significantly below the theoretical value of  $2.54 \mu_{\text{B}}$  calculated for the free ion in the  $L$ – $S$  coupling scheme. This effect clearly is a result of the covalency in the bonding interactions, as evidenced for **2** from the electronic structure calculations. Figure 5 shows the molecular orbitals of the five most energetic electrons. While SOMO–1 is a nondegenerate and almost pure f-orbital, HOMO–2/3’s, a set of close to doubly degenerate orbitals, are stabilized through a strong  $\pi$ -bonding interaction by approximately 190 kJ/mol. It clearly shows that the uranium–imido interaction in **2** is best described as a formal triple bond, consisting of two  $\pi$ -bonds and one  $\sigma$ -bond (the latter is not depicted).

An interesting feature of the triazacyclononane uranium(IV) complexes is the almost colorless appearance of solid samples. Similar to  $[(\text{ArO})_3\text{tacn}]\text{U}^{\text{IV}}(\text{OAr})$  (OAr = 2,4 di-*tert*-butyl phenolate) and  $[(\text{ArO})_3\text{tacn}]\text{U}^{\text{IV}}_2(\mu\text{-O})$ , which have been isolated as colorless and pale blue crystals, **3** is also colorless in the solid state. In contrast, the uranium(III) acetonitrile and the uranium(V) imido species **1b** and **2** are deep purple and green colored, respectively. This observation is also manifested in the complexes’ electronic absorption spectra. UV/vis/NIR spectra of solutions of **1a**, **1b**, and **2** display intense charge-transfer bands at 460, 500, and 400 nm ( $\epsilon = 2340, 500,$  and  $3800 \text{ M}^{-1} \text{ cm}^{-1}$ , see Supporting Information Figures S2, S3, and S4). Additional features in spectra of **1b** and **3** (Fig S5) include weak and sharp absorptions bands in the visible and near-infrared region between 500 and 2200 nm ( $\epsilon = 20$ – $100 \text{ M}^{-1} \text{ cm}^{-1}$ ), characteristic for f–f transitions typically found in actinide and especially lanthanide complexes.<sup>33</sup>

## Conclusion

In summary, the low-valent six- and seven-coordinate species  $[(\text{ArO})_3\text{tacn}]\text{U}$  and  $[(\text{ArO})_3\text{tacn}]\text{U}(\text{CH}_3\text{CN})$  with only one labile coordination site are potent precursors, allowing enhanced and controlled uranium reactivity. Utilizing the reactive nature of these compounds, we have synthesized and characterized a series of unprecedented uranium species in different oxidation states,  $[(\text{ArO})_3\text{tacn}]\text{U}^{\text{III}}(\text{CH}_3\text{CN})$ ,  $[(\text{ArO})_3\text{tacn}]\text{U}^{\text{IV}}(\text{N}_3)$ , and  $[(\text{ArO})_3\text{tacn}]\text{U}^{\text{V}}(\text{NSi}(\text{CH}_3)_3)$ . The coordination properties of this series of molecules provide interesting examples to illustrate the complexity of metal–ligand interactions found in uranium

(32) Note that the theoretical magnetic moment for an ion with an  $5f^3$  configuration ( $^4\text{I}_{9/2}$ ), like the metal centers in **1a** and **1b**, is only  $0.04 \mu_{\text{B}}$  higher at  $3.62 \mu_{\text{B}}$  as compared to  $3.58 \mu_{\text{B}}$  for an ion with two unpaired electrons and a  $^3\text{H}_4$  ground state as in **3**.

(33) Katz, J. J.; Morss, L. R.; Seaborg, G. T. *The Chemistry of the Actinide Elements*; Chapman Hall: New York, 1980.

coordination chemistry. The in-depth molecular and electronic structure examination of this series of complexes allowed for the identification of three types of bonding interactions in these complexes: (1) The polyamine ligand is weakly coordinated, and the metal–ligand interaction can be described as purely electrostatic. This type of bonding is typically found in main group-, lanthanide-, and trans-uranium metal chemistry. (2) The aryloxy–uranium bonds are also electrostatic in nature, but exceptionally strong  $\sigma$ -type bonds make the aryloxy a good, and in contrast to transition metal chemistry, redox-innocent ligator for uranium chemistry. (3) Most importantly, the acetonitrile and imido–uranium bonds display strong covalent interactions, manifested in marked  $\pi$ -bonding similar to that in transition metal complexes.

Reactivity studies on transformation reactions of the azido and imido species are currently under investigation.

## Experimental Section

**General Methods.** All experiments were performed under a dry nitrogen atmosphere using standard Schlenk techniques or an MBraun inert-gas glovebox. Solvents were purified using a two-column solid-state purification system (Glasscontour System, Irvine, CA) and transferred to the glovebox without exposure to air. NMR solvents were obtained from Cambridge Isotope Laboratories, degassed, and stored over activated molecular sieves prior to use.

**Methods.** Magnetization of crystalline powdered samples were recorded with a SQUID magnetometer (Quantum Design) at 10 kOe between 5 and 350 K for **1b**, and 5 and 300 K for samples **1a**, **2**, and **3**, respectively. Values of the magnetic susceptibility were corrected for the underlying diamagnetic increment ( $\chi_{\text{dia}} = -815 \times 10^{-6} \text{ cm}^3 \text{ mol}^{-1}$  (**1b**),  $-809 \times 10^{-6} \text{ cm}^3 \text{ mol}^{-1}$  (**2**),  $-815 \times 10^{-6} \text{ cm}^3 \text{ mol}^{-1}$  (**3**)) by using tabulated Pascal constants and the effect of the blank sample holders (gelatine capsule/straw). Samples used for magnetization measurement were recrystallized multiple times and checked for chemical composition and purity by elemental analysis (C, H, and N) and  $^1\text{H}$  NMR spectroscopy. Data reproducibility was also carefully checked.

Density functional theory calculations on **1b**, **2**, **3** were performed using the ADF2002.01 program suite.<sup>36–38</sup> The ADF package was utilized for geometry optimization of the core (all carbon atoms linking the six ligating nitrogen and oxygen atoms as well as the entire axial ligand:  $\text{CH}_3\text{CN}$ ,  $\text{N}_3^-$ , and  $(\text{CH}_3)_3\text{SiN}^{2-}$ ). All-electrons ZORA type V-basis sets were used for all atoms. The Vosko, Wilk, and Nusair (VWN) local density approximation was used. Becke's (1988) exchange correlation and Perdew (1986) correlation for the gradient correction were also used. The spin-unrestricted option was utilized together with ZORA relativistic formalism. No symmetry was specified in the calculation starting from the X-ray refined geometry of the seven-coordinate species. U represents the triple- $\zeta$  basis set with polarization and frozen core 5d. N represents the triple- $\zeta$  basis set with polarization and frozen core 1s. O represents the triple- $\zeta$  basis set with polarization and frozen core 1s. C represents the triple- $\zeta$ -basis set with polarization and frozen core 1s. H represents the triple- $\zeta$  basis set with polarization including H-polarization.

$^1\text{H}$  NMR spectra (300 or 400 MHz) were recorded at a probe temperature of 20 °C on Varian (Mercury 300/400) in  $\text{C}_6\text{D}_6$ . Chemical shifts were referenced to protio solvent impurities ( $\delta$  7.15 ( $\text{C}_6\text{D}_6$ )) and are reported in ppm.

Infrared spectra (400–4000  $\text{cm}^{-1}$ ) of solid samples were obtained on a Thermo Nicolet Avatar 360 FT-IR spectrophotometer as KBr pellets.

Electronic absorption spectra were recorded from 200 to 2500 nm (Shimadzu (UV-3101PC)) or from 190 to 820 (HP 8452A Diode Array) on a UV/vis/NIR spectrophotometer.

Results from elemental analysis were obtained from Kolbe Microanalytical Laboratory (Muelheim/Ruhr, Germany).

**Starting Materials.**  $[(\text{THF})_4\text{UI}_3]$  and  $[\text{U}(\text{N}(\text{Si}(\text{CH}_3)_2)_2)_3]$  were prepared as described by Clark et al.<sup>12,34,35</sup> Uranium turnings were purchased from Alfa Aesar and activated according to literature proceedings. Trityl azide (95%, Pfalz & Brauer, Inc.), 1-azidoadamantane (97%, Aldrich), and azidotrimethylsilane (97%, Acros, Organic) were obtained from commercial sources and used as received.

**Complex Synthesis.  $[(\text{ArO})_3\text{tacn}]\text{U}$  (**1a**).** A solution of  $[\text{U}(\text{N}(\text{SiMe}_3)_2)_3]$  (1.5 g, 2.09 mmol) in hexane (17 mL) was added to a solution of 1,4,7-tris(3,5-di-*tert*-butyl-2-hydroxybenzyl)-1,4,7-triazacyclononane ( $(\text{ArO})_3\text{tacn}$ ) (1.55 g, 1.98 mmol) in hexane (20 mL) and stirred for 12 h at room temperature. The resulting red-brown solution was filtered and stored at  $-40$  °C. Within 12 h, a red-brown microcrystalline precipitate formed, was filtered, washed with cold hexane, and dried in a vacuum (yield: 1.39 g, 1.36 mmol, 69%).  $^1\text{H}$  NMR (400 MHz, benzene- $d_6$ , 20 °C):  $\delta$  = 12.19 (s, 1H,  $\Delta\nu_{1/2}$  = 15.7 Hz), 9.05 (s, 1H,  $\Delta\nu_{1/2}$  = 12.7), 4.15 (s, 9H,  $\Delta\nu_{1/2}$  = 15.6 Hz), 2.63 (s, 9H,  $\Delta\nu_{1/2}$  = 7.08 Hz),  $-1.53$  (s, 1H,  $\Delta\nu_{1/2}$  = 41.4 Hz),  $-4.01$  (s, 1H,  $\Delta\nu_{1/2}$  = 20.8 Hz),  $-7.43$  (s, 1H,  $\Delta\nu_{1/2}$  = 23.7 Hz),  $-12.41$  (s, 1H,  $\Delta\nu_{1/2}$  = 44.1 Hz),  $-18.98$  (s, 1H,  $\Delta\nu_{1/2}$  = 32.9 Hz),  $-21.84$  (s, 1H,  $\Delta\nu_{1/2}$  = 45.1 Hz); elemental analysis (%) calcd for **1a**, C 60.10, H 4.12, N 7.71; found, C 60.02, H 4.18, N 7.84.

**$[(\text{ArO})_3\text{tacn}]\text{U}(\text{NCCH}_3)$  (**1b**).** A solution of **1a** (200 mg, 0.20 mmol) in acetonitrile (5 mL) was stirred at room temperature for 2 h. The resulting purple precipitate of  $[(\text{ArO})_3\text{tacn}]\text{U}(\text{NCCH}_3)$  (**1b**) was filtered, washed with cold acetonitrile, and dried in a vacuum (yield: 184 mg, 0.17 mmol, 88.5%). Recrystallization of the crude product from a saturated solution of acetonitrile at  $-40$  °C yielded needle-shaped crystals of **1b**·2 $\text{CH}_3\text{CN}$  suitable for X-ray diffraction analysis.  $^1\text{H}$  NMR (400 MHz, benzene- $d_6$ , 20 °C):  $\delta$  = 15.75 (s, H,  $\Delta\nu_{1/2}$  = 25.2 Hz), 11.29 (s, H,  $\Delta\nu_{1/2}$  = 16.5), 8.66 (s, H,  $\Delta\nu_{1/2}$  = 13.3 Hz), 4.15 (s, 9H,  $\Delta\nu_{1/2}$  = 16.4 Hz), 2.31 (s, 9H,  $\Delta\nu_{1/2}$  = 6.6 Hz), 0.70 (s, H,  $\Delta\nu_{1/2}$  = 22.2 Hz),  $-1.22$  (s, H,  $\Delta\nu_{1/2}$  = 22.6 Hz),  $-10.67$  (s, H,  $\Delta\nu_{1/2}$  = 14.6 Hz),  $-12.53$  (s, H,  $\Delta\nu_{1/2}$  = 23.5 Hz),  $-17.70$  (s, H,  $\Delta\nu_{1/2}$  = 36.4 Hz),  $-19.14$  (s, H,  $\Delta\nu_{1/2}$  = 32.8 Hz); elemental analysis (%) calcd for **1b**, C 60.04, H 7.70, N 5.28; found, C 59.85, H 7.62, N 5.17.

**$[(\text{ArO})_3\text{tacn}]\text{U}(\text{N}(\text{Si}(\text{CH}_3)_3))$  (**2**).** A cold solution of trimethylsilyl azide (23.6 mg, 0.20 mmol) was added dropwise to a solution of **1a** (200 mg, 0.20 mmol) in 7 mL of hexane. Upon addition, a green solution was obtained followed by the formation of a colorless precipitate  $[(\text{ArO})_3\text{tacn}]\text{U}(\text{N}_3)$  (**3**). After the precipitate was filtered and the solids were washed with pentane, the filtrate was evaporated to dryness and recrystallized from acetonitrile to yield green crystals of  $[(\text{ArO})_3\text{tacn}]\text{U}(\text{N}(\text{Si}(\text{CH}_3)_3))$  (**2**) (yield: 85 mg, 0.08 mmol, 39%). Recrystallization of **2** from a saturated solution of hexane at room temperature yielded green rectangular plates of **2**· $\frac{1}{2}\text{C}_6\text{H}_{14}$  suitable for X-ray diffraction analysis.  $^1\text{H}$  NMR (300 MHz, benzene- $d_6$ , 20 °C):  $\delta$  = 49.5 (s, H,  $\Delta\nu_{1/2}$  = 23.0 Hz), 23.74 (s, H,  $\Delta\nu_{1/2}$  = 12.8 Hz), 22.0 (s, H,  $\Delta\nu_{1/2}$  = 12.8 Hz), 20.61 (s, H,  $\Delta\nu_{1/2}$  = 37.2 Hz), 2.02 (s, H,  $\Delta\nu_{1/2}$  = 11.35 Hz),  $-0.85$  (s, 9H,  $\Delta\nu_{1/2}$  = 4.0),  $-4.44$  (s, 3H,  $\Delta\nu_{1/2}$  = 4.5 Hz),  $-4.73$  (s, 6H,  $\Delta\nu_{1/2}$  = 43.2 Hz),  $-14.75$  (s, H,  $\Delta\nu_{1/2}$  = 19.9 Hz); elemental analysis (%) calcd for **2**, C 58.62, H 7.93, N 5.06; found, C 58.55, H 7.86, N 4.95.

**$[(\text{ArO})_3\text{tacn}]\text{U}(\text{N}_3)$  (**3**).** Method A: The procedure described for the synthesis of **2** was followed for preparation of **3**. The colorless

(34) Avens, L. R.; Bott, S. G.; Clark, D. L.; Sattelberger, A. P.; Watkin, J. G.; Zwick, B. D. *Inorg. Chem.* **1994**, *33*, 2248–2256.

(35) Clark, D. L.; Sattelberger, A. P.; Bott, S. G.; Vrtis, R. N. *Inorg. Chem.* **1989**, *28*, 1771–1773.

(36) Velde, G. T.; Bickelhaupt, F. M.; Baerends, E. J.; Guerra, C. F.; Van Gisbergen, S. J. A.; Snijders, J. G.; Ziegler, T. *J. Comput. Chem.* **2001**, *22*, 931–967.

(37) Guerra, C. F.; Snijders, J. G.; te Velde, G.; Baerends, E. J. *Theor. Chem. Acc.* **1998**, *99*, 391–403.

(38) ADF 2002.01, SCM, Theoretical Chemistry, Vrije Universiteit, Amsterdam, The Netherlands.



precipitate of **3** was collected by filtration, washed with pentane, and dried in a vacuum (yield: 30 mg, 0.03 mmol, 14%).

Method B: Complex **3** can also be synthesized using **1b** as a starting material. Trimethylsilyl azide (10.9 mg, 0.094 mmol) was added dropwise via syringe to 100 mg of **1b** (0.094 mmol) dissolved in CH<sub>3</sub>CN (4 mL). Upon addition, the deeply purple colored solution of **1b** discolored with formation of a white precipitate. The precipitate was filtered, washed with pentane, and dried in a vacuum (yield: 70 mg, 0.065 mmol, 70%).

Recrystallization of **3** from a saturated solution of hexane at room temperature yielded colorless, irregular-shaped crystals **3**·C<sub>6</sub>H<sub>14</sub> suitable for X-ray diffraction analysis. <sup>1</sup>H NMR (300 MHz, benzene-*d*<sub>6</sub>, 20 °C): δ = 22.49 (s, H, Δ*v*<sub>1/2</sub> = 22.8 Hz), 18.49 (s, H, Δ*v*<sub>1/2</sub> = 19.9 Hz), 3.21 (s, H, Δ*v*<sub>1/2</sub> = 5.1 Hz), -0.93 (s, 9H, Δ*v*<sub>1/2</sub> = 3.3 Hz), -3.36 (s, 9H, Δ*v*<sub>1/2</sub> = 5.3 Hz), -4.46 (s, H, Δ*v*<sub>1/2</sub> = 2.9 Hz), -5.18 (s, H, Δ*v*<sub>1/2</sub> = 21.0 Hz), -6.86 (s, H, Δ*v*<sub>1/2</sub> = 12.4 Hz), -12.91 (s, H, Δ*v*<sub>1/2</sub> = 6.5 Hz), -14.81 (s, H, Δ*v*<sub>1/2</sub> = 14.4 Hz), -52.48 (s, H, Δ*v*<sub>1/2</sub> = 11.0 Hz). IR spectrum (KBr): ν<sub>as</sub>(U–N<sub>3</sub>) = 2080 cm<sup>-1</sup>; elemental analysis (%) calcd for **3**, C 58.08, H 7.50, N 7.82; found, C 58.21, H 7.39, N 7.81.

**Crystallographic Details.** Crystallographic details for **1b**: Purple needle-shaped crystals grown from a concentrated solution of [(ArO<sub>3</sub>-tacn)U] in CD<sub>3</sub>CN at room temperature were coated with Paratone N oil on a microscope slide. A crystal of approximate dimensions 0.30 × 0.04 × 0.04 mm<sup>3</sup> was selected and mounted on a glass fiber. A total of 32 724 reflections (-16 ≤ *h* ≤ 16, -41 ≤ *k* ≤ 41, -10 ≤ *l* ≤ 10) were collected at *T* = 100(2) K in the θ range from 1.31 to 22.50°, of which 7452 were unique (*R*<sub>int</sub> = 0.0740); Mo Kα radiation (λ = 71 073 Å). The structure was solved by Direct Methods (Shelxtl Version 6.10, Bruker AXS, Inc., 2000). With the exception of solvent and hydrogen atoms, all atoms were refined anisotropically. Hydrogen atoms were placed in calculated idealized positions. The residual peak and hole electron density were 1.843 and -1.570 e Å<sup>-3</sup>. The absorption coefficient was 2.887 mm<sup>-1</sup>. The least-squares refinement converged normally with residuals of *R*<sub>1</sub> = 0.0687 (all data), *wR*<sub>2</sub> = 0.0935, and GOF = 1.031 (*I* > 2σ(*I*)). C<sub>57</sub>H<sub>87</sub>N<sub>6</sub>O<sub>3</sub>U, space group *P*2<sub>1</sub>/*c*, monoclinic, *a* = 15.5674(15), *b* = 38.892(4), *c* = 9.4511(9), β = 93.495(2)°, *V* = 5711.4(10) Å<sup>3</sup>, *Z* = 4, ρ<sub>calcd</sub> = 1.329 mg/m<sup>3</sup>, *F*(000) = 2348, *R*(*F*) = 0.0459, *wR*(*F*<sup>2</sup>) = 0.0894. CCDC reference number: 192192.

Crystallographic details for **2**: Green rectangular plates grown from a solution of hexane at room temperature were coated with Paratone N oil on a microscope slide. A crystal of approximate dimensions 0.40 × 0.24 × 0.05 mm<sup>3</sup> was selected and mounted on a glass fiber. A total of 66 403 reflections (-28 ≤ *h* ≤ 28, -16 ≤ *k* ≤ 16, -30 ≤ *l* ≤ 30) were collected at *T* = 100(2) K in the θ range from 1.45 to 22.50°, of which 15 297 were unique (*R*<sub>int</sub> = 0.0549); Mo Kα radiation (λ = 71 073 Å). The structure was solved by Direct Methods (Shelxtl Version

6.10, Bruker AXS, Inc., 2000). With the exception of one *tert*-butyl group and the hydrogen atoms, all atoms were refined anisotropically. Hydrogen atoms were placed in idealized positions. The residual peak and hole electron density was 2.364 and -0.835 e Å<sup>-3</sup>. The absorption coefficient was 2.840 mm<sup>-1</sup>. The least-squares refinement converged normally with residuals of *R*<sub>1</sub> = 0.0517 (all data), *wR*<sub>2</sub> = 0.0803, and GOF = 0.917 (*I* > 2σ(*I*)). C<sub>114</sub>H<sub>188</sub>N<sub>8</sub>O<sub>6</sub>Si<sub>2</sub>U<sub>2</sub>, space group *P*2<sub>1</sub>/*n*, monoclinic, *a* = 26.853(2), *b* = 15.5322(13), *c* = 28.082(2) Å, β = 93.6170(10)°, *V* = 11689.2(17) Å<sup>3</sup>, *Z* = 4, ρ<sub>calcd</sub> = 1.306 mg/m<sup>3</sup>, *F*(000) = 4752, *R*(*F*) = 0.0342, *wR*(*F*<sup>2</sup>) = 0.0769. CCDC reference number: 192194.

Crystallographic details for **3**: Colorless irregular-shaped crystals grown from a solution of hexane at room temperature were coated with Paratone N oil on a microscope slide. A crystal of approximate dimensions 0.16 × 0.10 × 0.02 mm<sup>3</sup> was selected and mounted on a glass fiber. A total of 36 975 reflections (-15 ≤ *h* ≤ 15, -21 ≤ *k* ≤ 21, -25 ≤ *l* ≤ 25) were collected at *T* = 100(2) K in the θ range from 1.34 to 22.50°, of which 8958 were unique (*R*<sub>int</sub> = 0.1225); Mo Kα radiation (λ = 71 073 Å). The structure was solved by Direct Methods (Shelxtl Version 6.10, Bruker AXS, Inc., 2000). With the exception of N(4), solvent, and hydrogen atoms, all atoms were refined anisotropically. Hydrogen atoms were placed in idealized positions. The residual peak and hole electron density were 2.592 and -1.979 e Å<sup>-3</sup>. The absorption coefficient was 2.405 mm<sup>-1</sup>. The least-squares refinement converged normally with residuals of *R*<sub>1</sub> = 0.1117 (all data), *wR*<sub>2</sub> = 0.1734, and GOF = 1.015 (*I* > 2σ(*I*)). C<sub>57</sub>H<sub>92</sub>N<sub>6</sub>O<sub>3</sub>U, space group *P*2<sub>1</sub>/*n*, monoclinic, *a* = 14.563(5), *b* = 19.866(7), *c* = 24.082(8) Å, β = 100.187(5)°, *V* = 6858(4) Å<sup>3</sup>, *Z* = 4, ρ<sub>calcd</sub> = 1.111 mg/m<sup>3</sup>, *F*(000) = 2368, *R*(*F*) = 0.0655, *wR*(*F*<sup>2</sup>) = 0.1525. CCDC reference number: 192193.

**Acknowledgment.** This work was supported by the University of California, San Diego. I.C.-R. thanks the National Institute of Health for a fellowship (3 T32 DK07233-2651). We are grateful to the University of Copenhagen (Denmark) for granting leave of absence to K.O. K.O. thanks the Danish Chemical Society for financial support. We dedicate this work to the memory of Prof. Richard Koerner.

**Supporting Information Available:** Complete crystallographic details of the X-ray structures of **1b**, **2**, and **3** and electronic absorption spectra of **1b**, **2**, and **3**, as well as the molecular orbital diagram and the Mulliken population of **3** (PDF and CIF). This material is available free of charge via the Internet at <http://pubs.acs.org>.

JA028342N